Pattern Formation and Chaos

Insights from Large Scale Numerical Simulations of Rayleigh-Bénard Convection

Collaborators: Mark Paul, Keng-Hwee Chiam, Janet Scheel, Henry Greenside, Anand Jayaraman, Paul Fischer

Support: DOE; Computer time: NSF, NERSC, NCSA, ANL

Outline

Use numerical simulation of Rayleigh-Bénard convection in realistic geometries to learn about complex spatial patterns and dynamics in spatially extended systems.

Examples:

- Pattern chaos
- Role of mean flow
- Lyapunov exponents and vectors
- Domain chaos: scaling and discrepancies between theory and experiment

Rayleigh-Bénard Convection

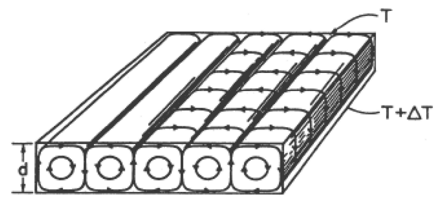

RBC allows a *quantitative* comparison to be made between theory and experiment.

Nondimensional Boussinesq Equations

- Momentum Conservation

$$\frac{1}{\sigma}\left[\frac{\partial\vec{u}}{\partial t}+\left(\vec{u}\bullet\vec{\nabla}\right)\vec{u}\right]=-\vec{\nabla}p+R\,T\hat{e}_z+\nabla^2\vec{u}+2\Omega\hat{e}_z\times\vec{u}$$

- Energy Conservation

$$\frac{\partial T}{\partial t}+\left(\vec{u}\bullet\vec{\nabla}\right)T=\nabla^2 T$$

- Mass Conservation

$$\vec{\nabla}\bullet\vec{u}=0$$

Aspect Ratio: $\Gamma=\frac{r}{h}$

BC: no-slip, insulating or conducting, and constant ΔT

Spectral Element Numerical Solution

- Accurate simulation of long-time dynamics
- Exponential convergence in space, third order in time
- Efficient parallel algorithm, unstructured mesh
- Arbitrary geometries, realistic boundary conditions

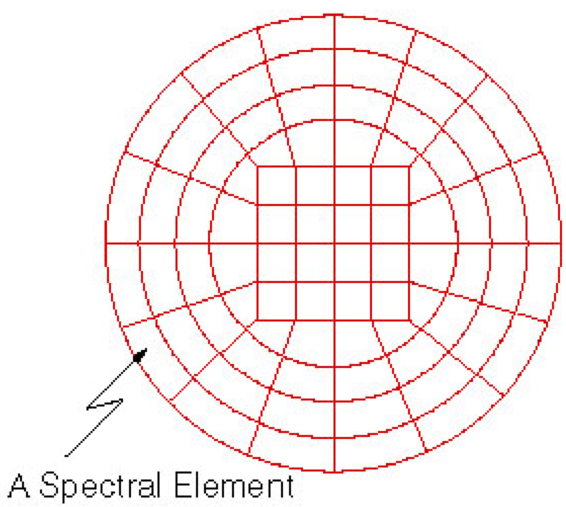

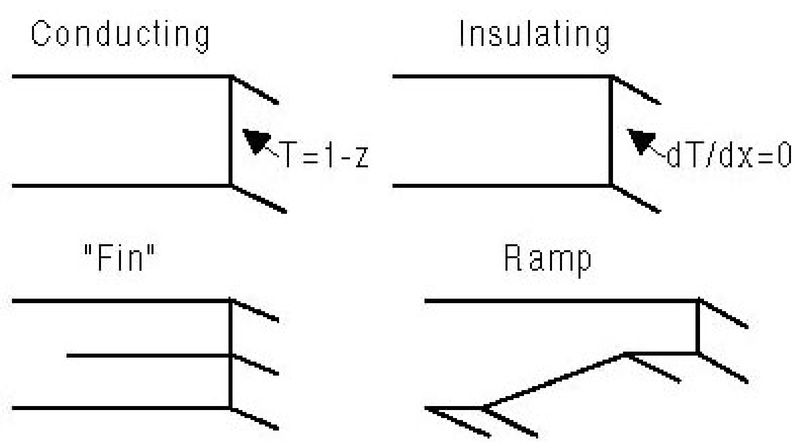

Convection in an elliptical container

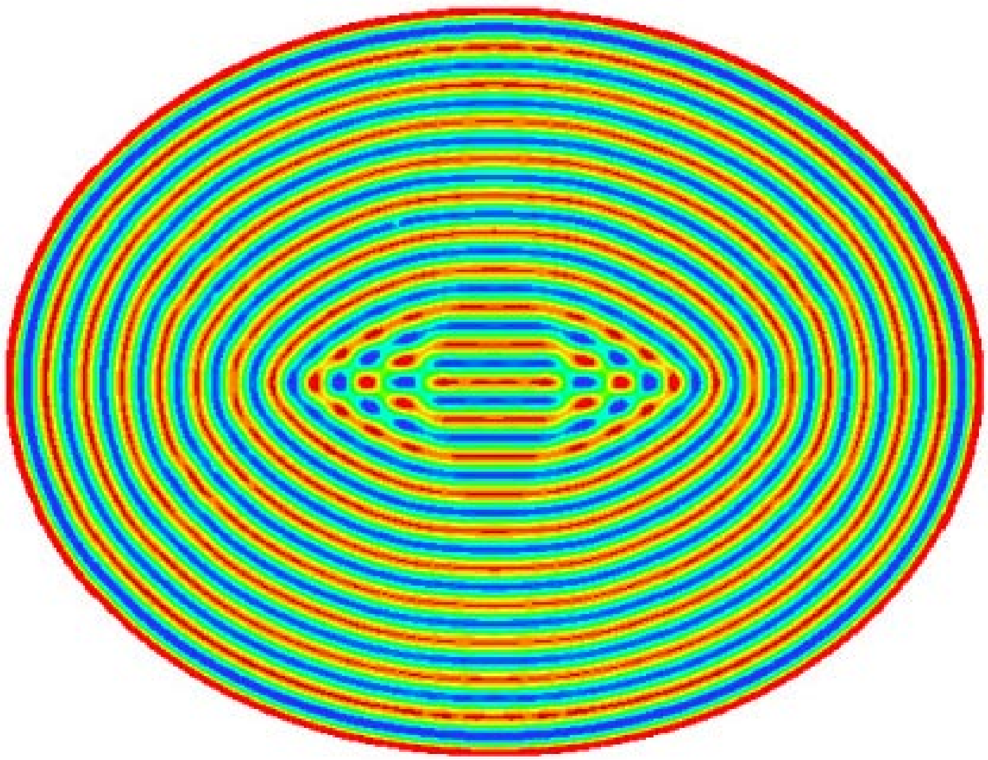

cf. Ercolani, Indik, and Newell, Physica D (2003)

How our simulations can complement experiments

- Knowledge of full flow field (e.g. mean flow) and other diagnostics (e.g. total heat flow)
- Measure quantities inaccessible to experiment e.g. Lyapunov exponents and vectors
- No experimental/measurement noise (roundoff "noise" very small)
- Readily tune parameters
- Turn on and off particular features of the physics (e.g. centrifugal effects, mean flow)
- Compare realistic and artificial (e.g. periodic) boundary conditions

Limitations

- System size and time of simulation limited in context of patterns/spatiotemporal chaos
- Results reflect a model of the real world (what you get out depends on what you put in)

Pattern chaos: convection in small cylindrical geometries

- First experiments: $\Gamma = 5.27$ cell, cryogenic (normal) liquid He^4 as fluid. High precision heat flow measurements (no flow visualization).
- Onset of aperiodic time dependence in low Reynolds number flow: relevance of chaos to "real" (continuum) systems.
- Power law decrease of power spectrum $P(f) \sim f^{-4}$

G. Ahlers, Phys. Rev. Lett. **30**, 1185 (1974)

G. Ahlers and R.P. Behringer, Phys. Rev. Lett. **40**, 712 (1978)

H. Gao and R.P. Behringer, Phys. Rev. A**30**, 2837 (1984)

V. Croquette, P. Le Gal, and A. Pocheau, Phys. Scr. T**13**, 135 (1986)

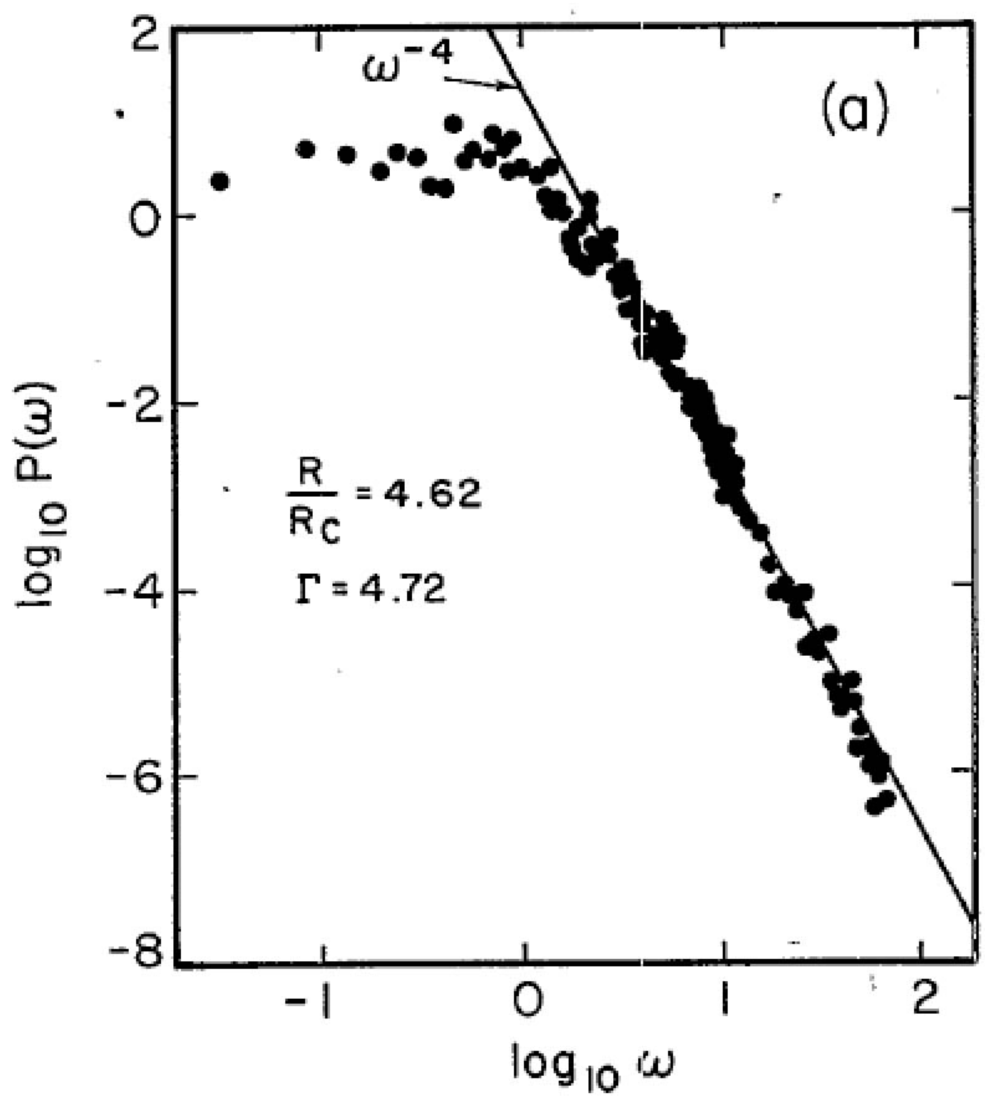

(from Ahlers and Behringer 1978)

Numerical Simulations

- $\Gamma = 4.72$, $\sigma = 0.78$, $2600 \lesssim R \lesssim 7000$
- Conducting sidewalls
- Random thermal perturbation initial conditions
- Simulation time $\sim 100\tau_h$
  - Simulation time $\sim$ 12 hours on 32 processors
  - Experiment time $\sim$ 172 hours or $\sim$ 1 week

$R = 3127$ $R = 6949$

Power Spectrum

- Simulations of low dimensional chaos (e.g. Lorenz model) show exponential decaying power spectrum
- Power law power spectrum easily obtained from stochastic models (white-noise driven oscillator, etc.)

Simulation yields a power law over the range accessible to experiment....

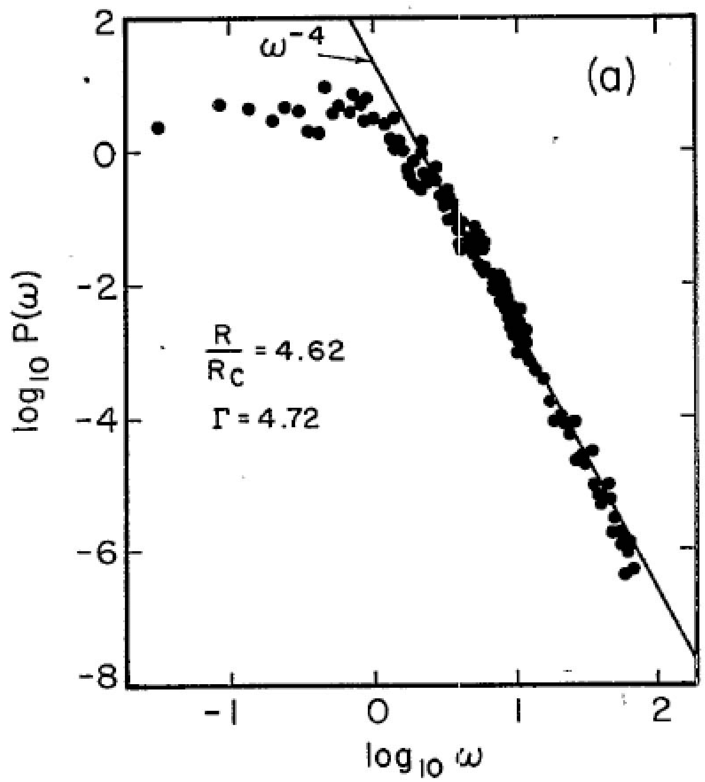

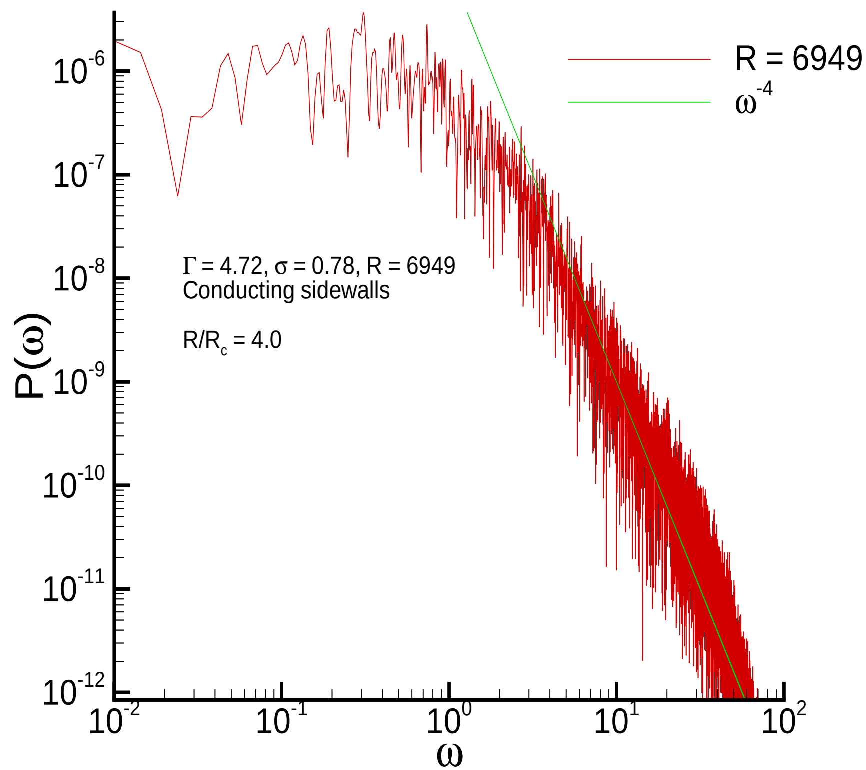

but when larger frequencies are included an exponential tail is found

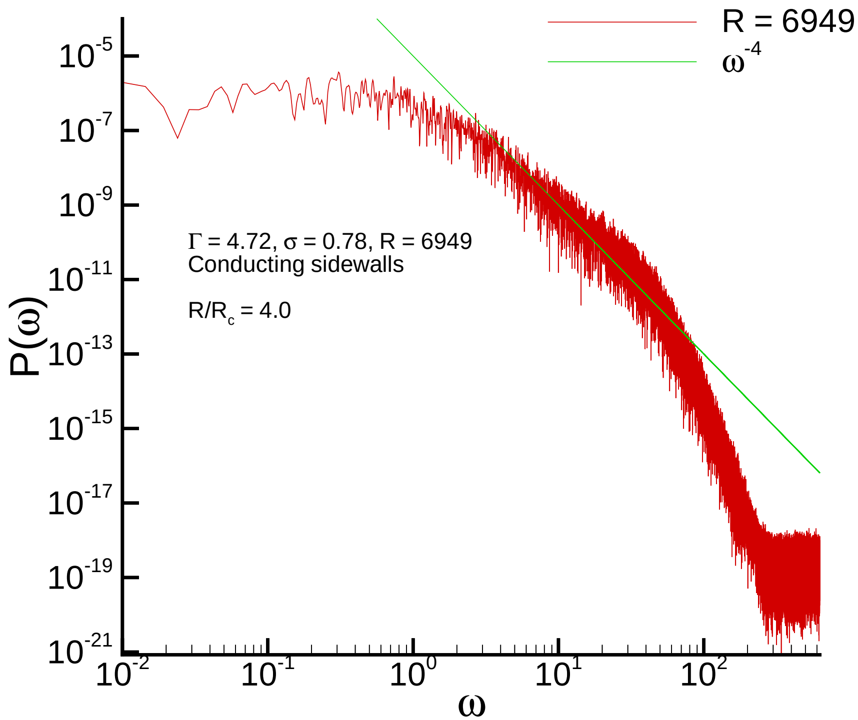

Exponential tail not seen in experiment because of instrumental noise floor

Where does the power law come from?

Power law arises from quasi-discontinuous changes in the slope of $N(t)$ on a $t = 0.1 - 1$ time scale associated with roll pinch-off events.

This is clearest to see for the low Rayleigh number where the motion is periodic, but again the power spectrum has a power law fall off.

Sharp events similar in chaotic and periodic signals

Spectrogram

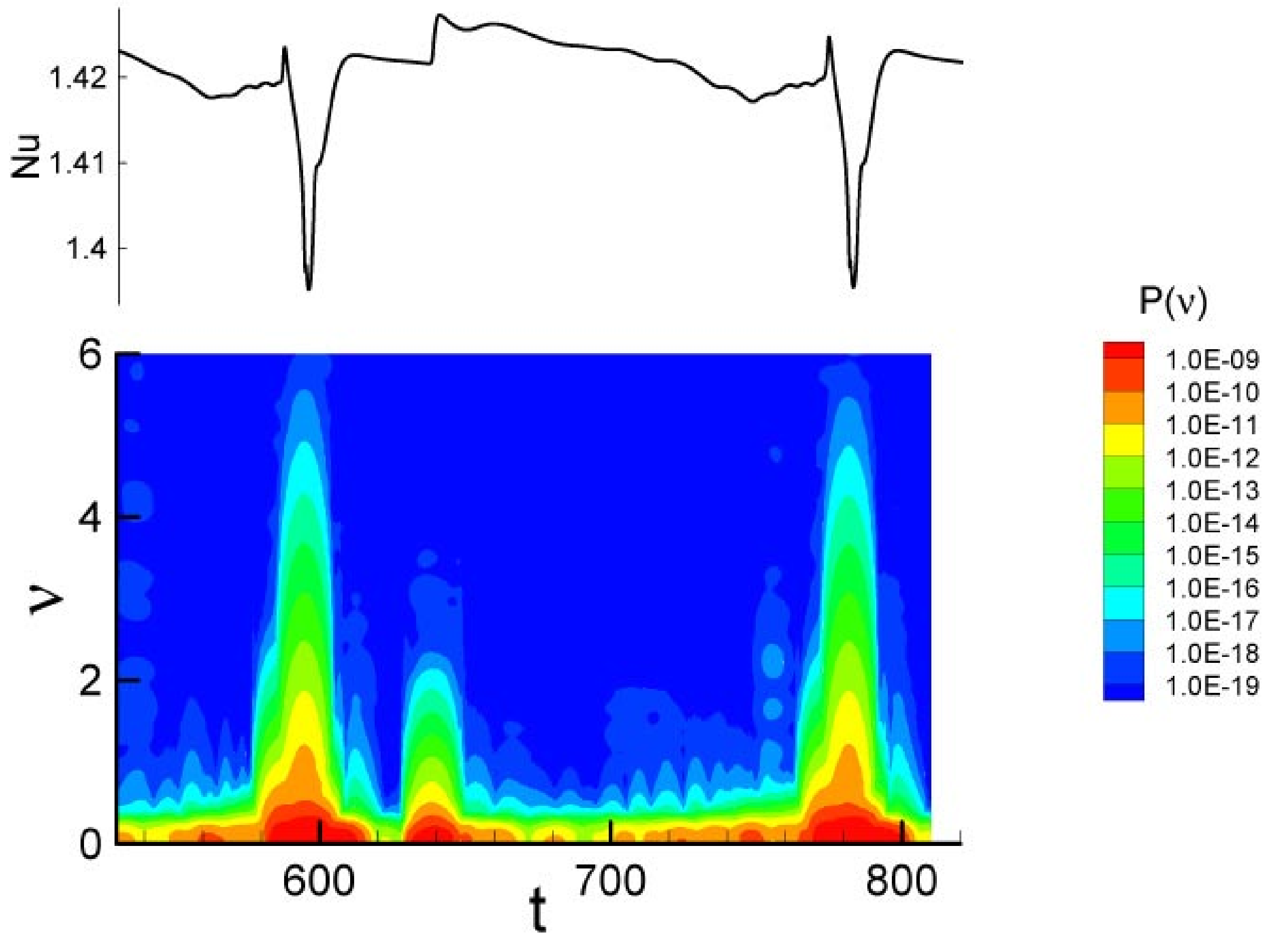

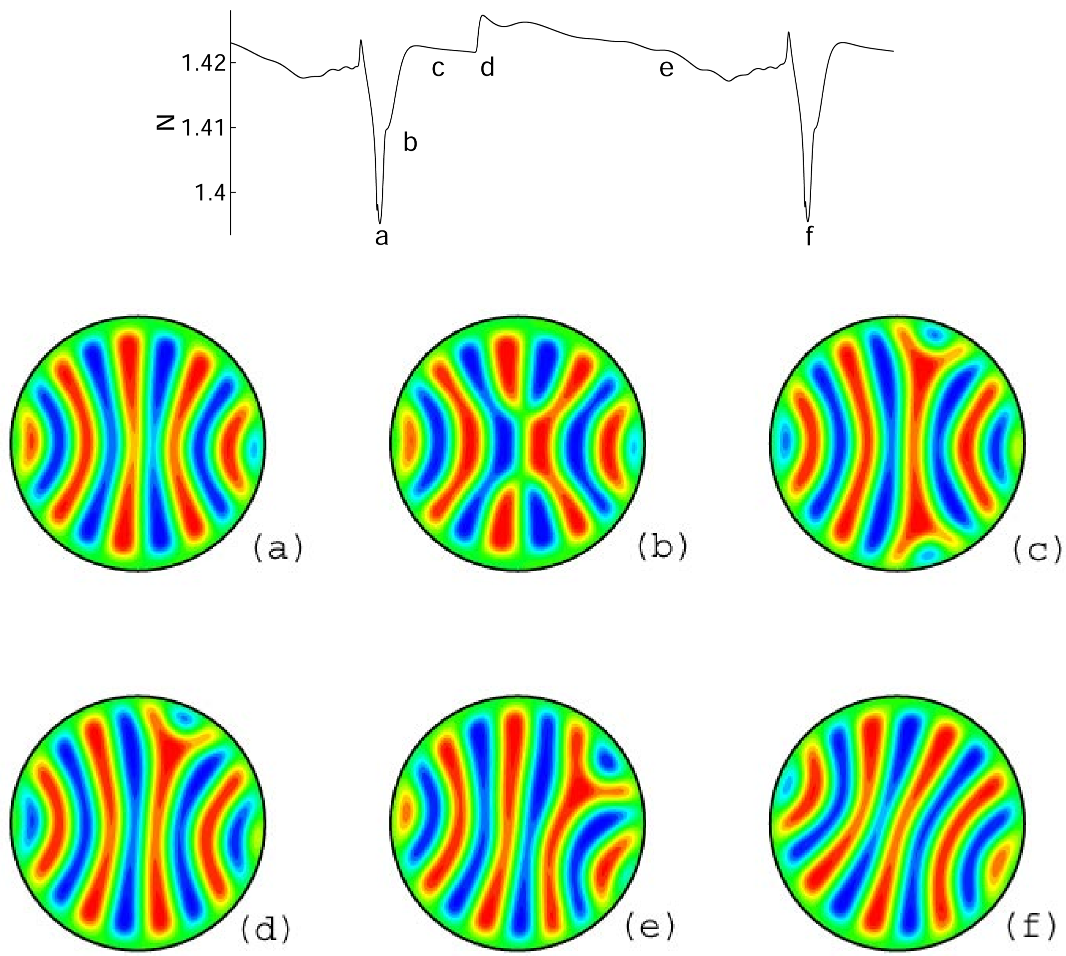
1.42
1.41
1.4
N
a
b
c
d
e
f
(a)
(b)
(c)
(d)
(e)
(f)

Mean Flow

What is mean flow?

Remember the fluid equations

$$\sigma^{-1}(\partial_t + \mathbf{u}\cdot\nabla)\,\mathbf{u} = -\nabla p + R T\hat{z} + \nabla^2\mathbf{u}$$

$$\nabla\cdot\mathbf{u} = 0$$

The pressure is a not an independent dynamical variable. It is determined implicitly to enforce the incompressibility

$$\nabla^2 p = -\sigma^{-1}\nabla\cdot[(\mathbf{u}\cdot\nabla)\mathbf{u}] + R\,\partial T/\partial z$$

Focussing on the nonlinear "Reynolds stress" term and writing $p = p_0(x, y) + \bar{p}(x, y, z)$

$$p_0(x, y) \sim \sigma^{-1}\int dx'dy'\,\ln(1/\left|\mathbf{r}-\mathbf{r}'\right|)\left\langle\nabla'\,[(\mathbf{u}\cdot\nabla)\mathbf{u}]\right\rangle_z$$

This gives a "singular" pressure term that depends on distant parts of the convection pattern.

Mean flow is driven by curvature of the rolls, compression of the rolls, and gradients of the amplitude.

The mean flow then advects the pattern giving additional slow time dependence.

Near threshold

$$\mathbf{U} = \text{solenoidal part of } \mathbf{k}\nabla_\perp \cdot (\mathbf{k}A^2)$$

Writing $\mathbf{U}$ in terms of a stream function ζ so that $\mathbf{U} = (-\partial_y \zeta, \partial_x \zeta)$

$$\omega = -\nabla_\perp^2 \zeta = -\gamma\, \hat{\mathbf{z}} \cdot \nabla_\perp \times [\mathbf{k}\nabla \cdot (\mathbf{k}A^2)]$$

Mean flow in cylindrical system chaos

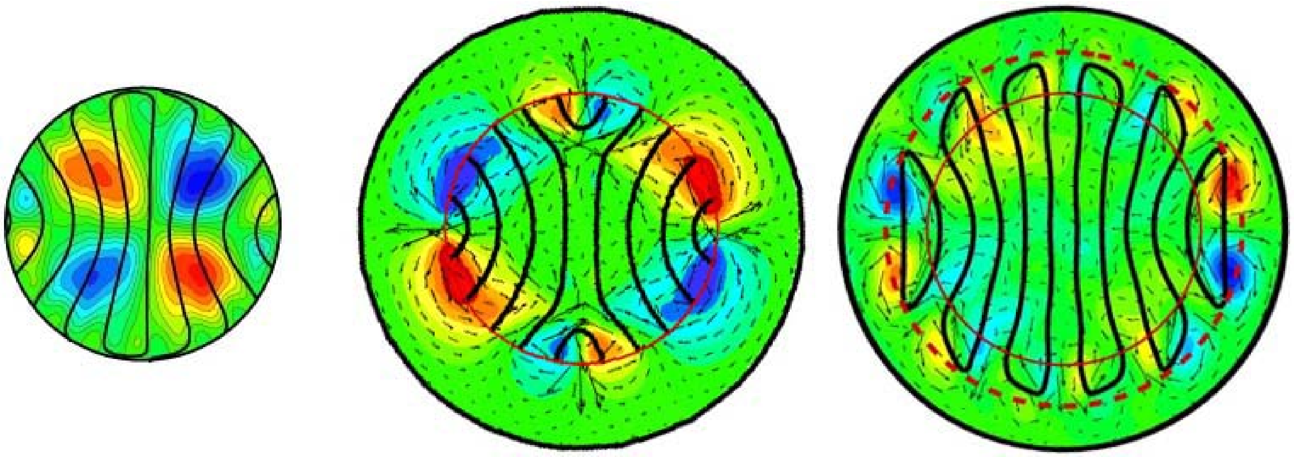

3 convection cells with different side wall conditions: (a) rigid; (b) finned; and (c) ramped. Case (a) is dynamic, the others static.

Patterns with and without mean flow

Mean flow and stationary patterns

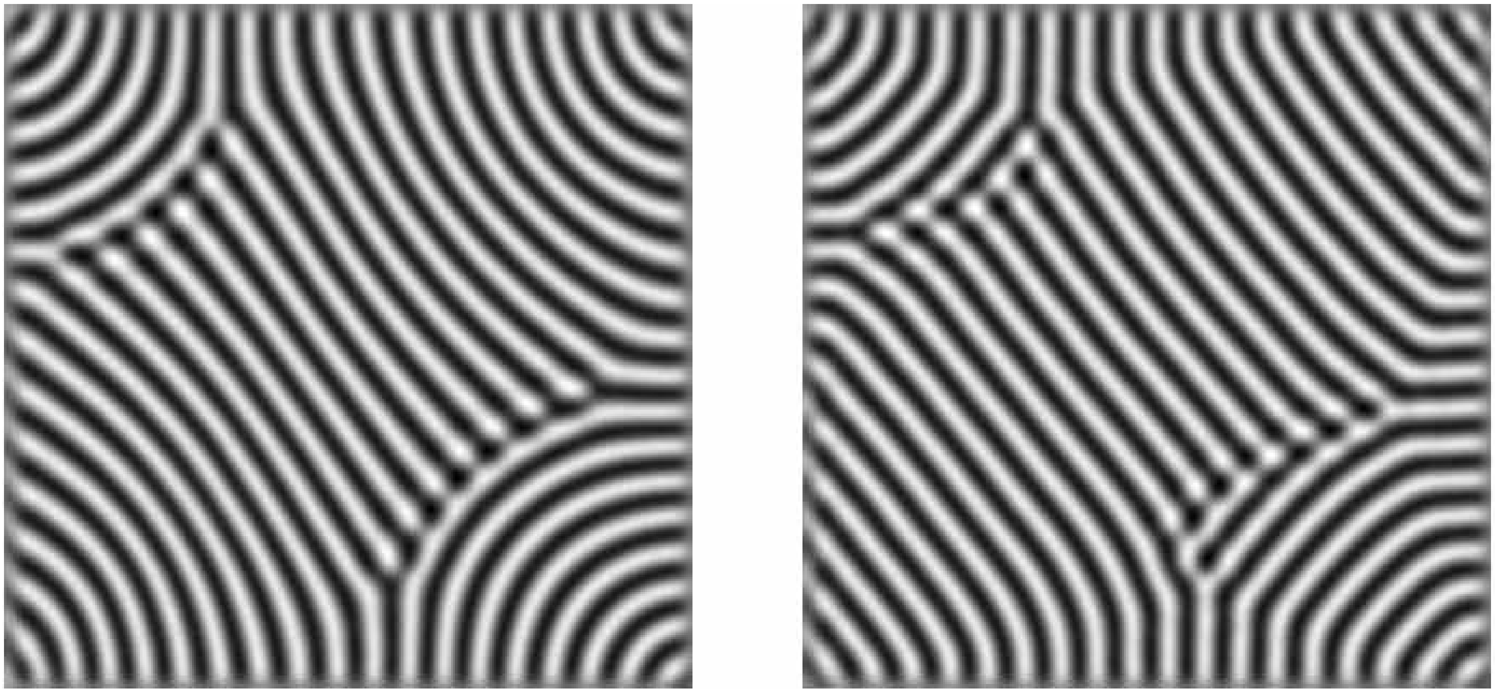

$\varepsilon = 0.15$, $\sigma = 1$ [From Keng-Hwee Chiam, Caltech thesis]

Wavenumber distribution

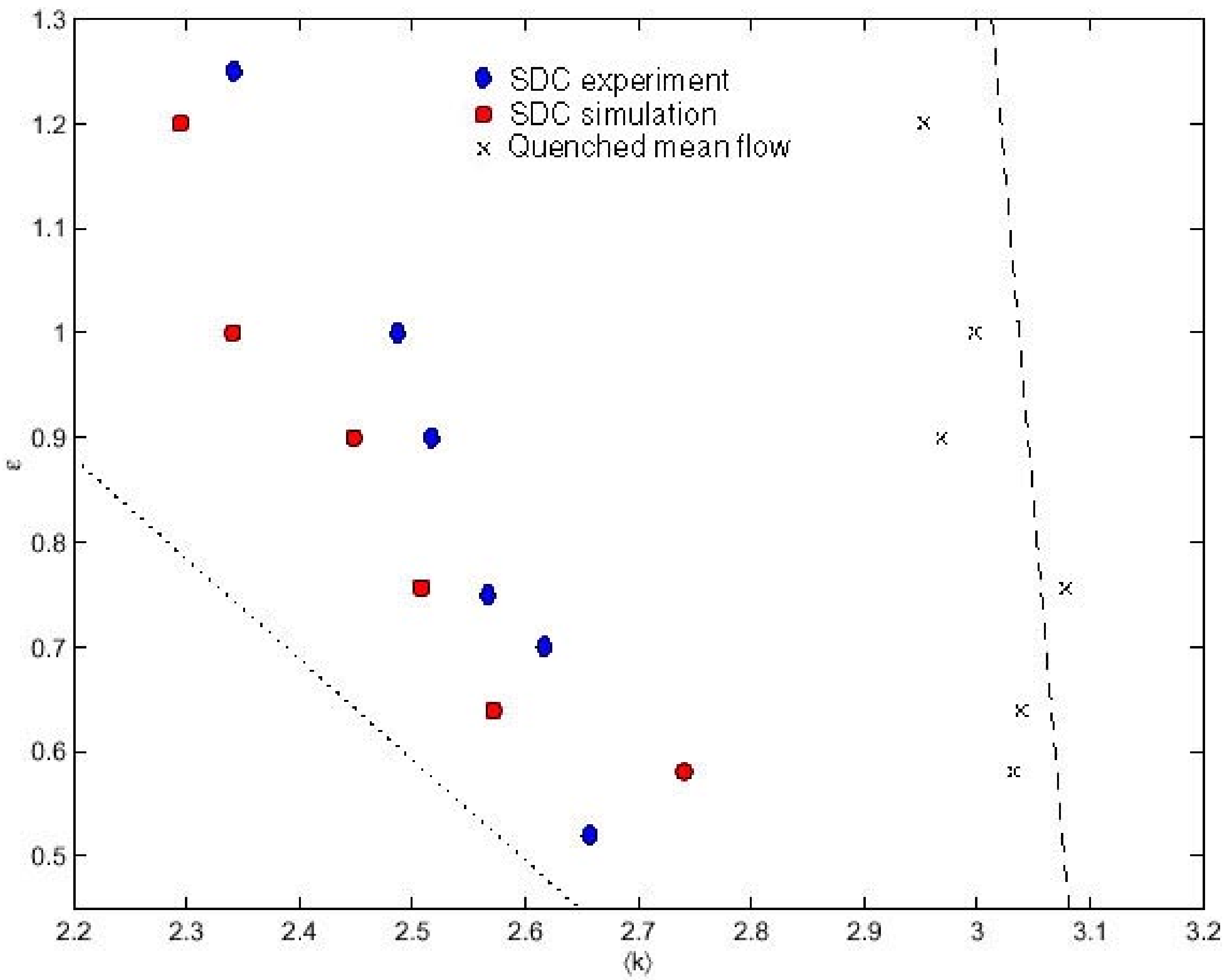

Mean flow favors normal alignment at boundaries

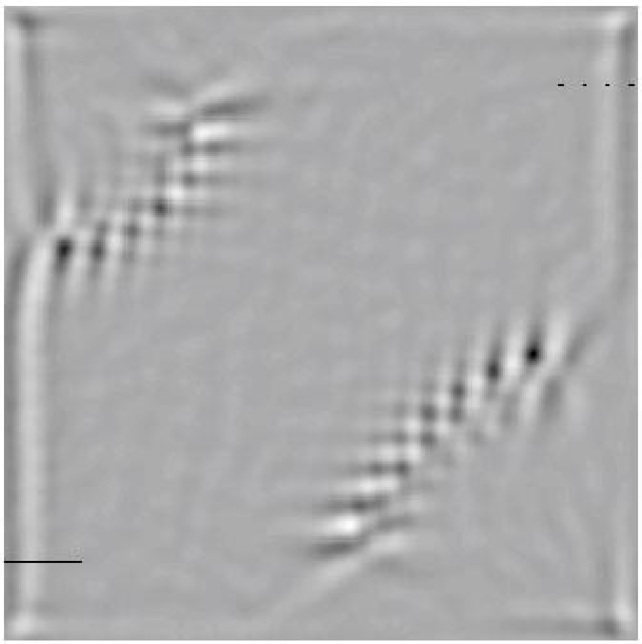

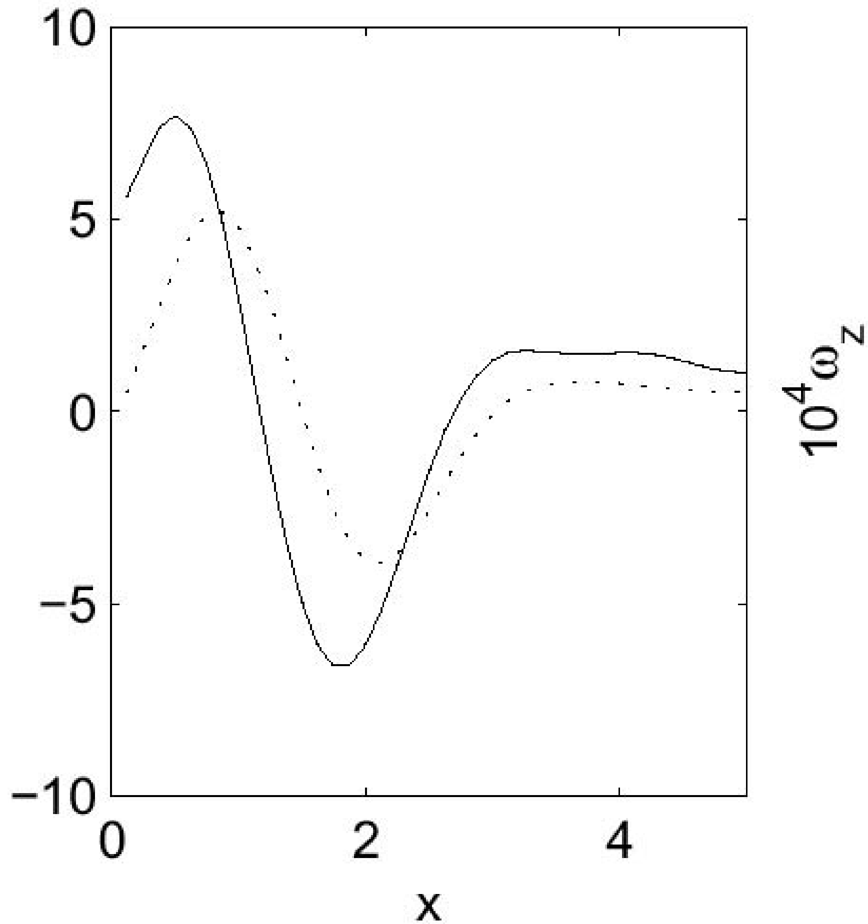

Sensitive dependence on initial conditions

- Lyapunov exponents:
  - ◇ Quantify the sensitivity to initial conditions
  - ◇ Define chaos
- Lyapunov vectors:
  - ◇ Associate sensitivity with specific events (defect creation, etc.)
  - ◇ Propagation of disturbances (Lorenz's question!)
- Lyapunov dimension:
  - ◇ Quantifies the number of active degrees of freedom
  - ◇ Scaling with system size may perhaps be used to define spatiotemporal chaos (microextensive chaos: Tajima and Greenside, 2002)

Lyapunov exponents

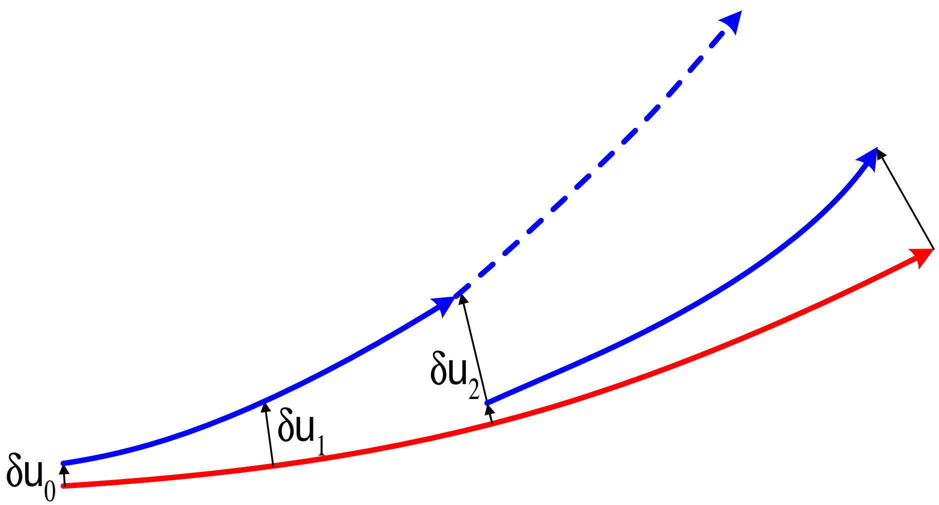

$$\delta u = \delta u_0 e^{\lambda_1 t}, \qquad \lambda_1 = \lim_{t\to\infty} \frac{1}{t} \ln \frac{\delta u}{\delta u_0}$$

Line lengths $\to e^{\lambda_1 t}$, Areas $\to e^{(\lambda_1+\lambda_2)t}$, Volumes $\to e^{(\lambda_1+\lambda_2+\lambda_3)t}, \ldots$

Lyapunov Dimension

$$D_L = \nu + \frac{1}{|\lambda_{\nu+1}|} \sum_{i=1}^{\nu} \lambda_i$$

where ν is the largest index such that the sum is positive.

Numerical Approach

Chaotic Boussinesq driving solution:

$$\frac{1}{\sigma}\left[\frac{\partial \vec{u}}{\partial t} + \left(\vec{u}\cdot\vec{\nabla}\right)\vec{u}\right] = -\vec{\nabla} p + RT\hat{e}_z + \nabla^2\vec{u}$$

$$\frac{\partial T}{\partial t} + \left(\vec{u}\cdot\vec{\nabla}\right)T = \nabla^2 T$$

$$\vec{\nabla}\cdot\vec{u} = 0$$

Linearized equations (tangent space equations):

$(\vec{u}, p, T) \rightarrow (\vec{u} + \delta\vec{u}_k, p + \delta p_k, T + \delta T_k)$, for $k = 1, \ldots, n$

$$\frac{1}{\sigma}\left[\frac{\partial \delta\vec{u}_k}{\partial t} + \left(\vec{u}\cdot\vec{\nabla}\right)\delta\vec{u}_k + \left(\delta\vec{u}_k\cdot\vec{\nabla}\right)\vec{u}\right] = -\vec{\nabla}\delta p_k + R\delta T\hat{e}_z + \nabla^2\delta\vec{u}_k$$

$$\frac{\partial \delta T_k}{\partial t} + \left(\vec{u}\cdot\vec{\nabla}\right)\delta T_k + \left(\delta\vec{u}_k\cdot\vec{\nabla}\right)T = \nabla^2\delta T_k$$

$$\vec{\nabla}\cdot\delta\vec{u}_k = 0$$

Small system Lyapunov exponent…

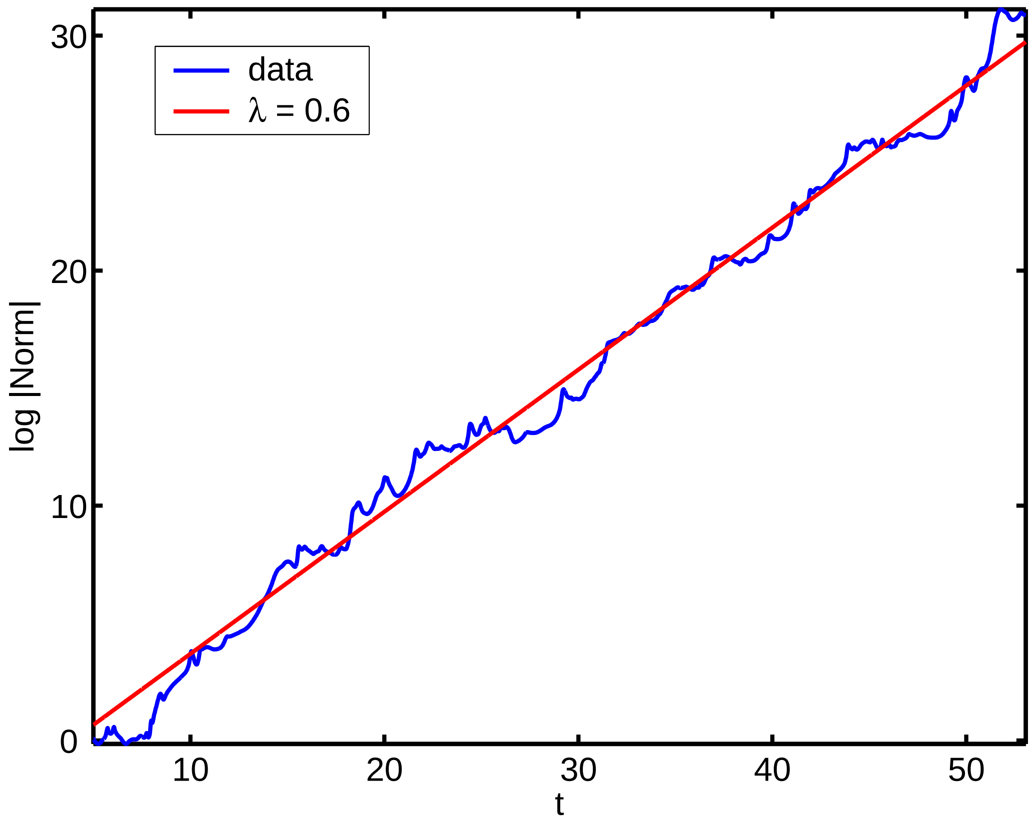

Aspect ratio $\Gamma = 4.7$, $R = 6950$.

…and Lyapunov vector

Lyapunov vector for spiral defect chaos

(from Keng-Hwee Chiam, Caltech thesis 2003, after Egolf et al.)

Scaling near onset of domain chaos

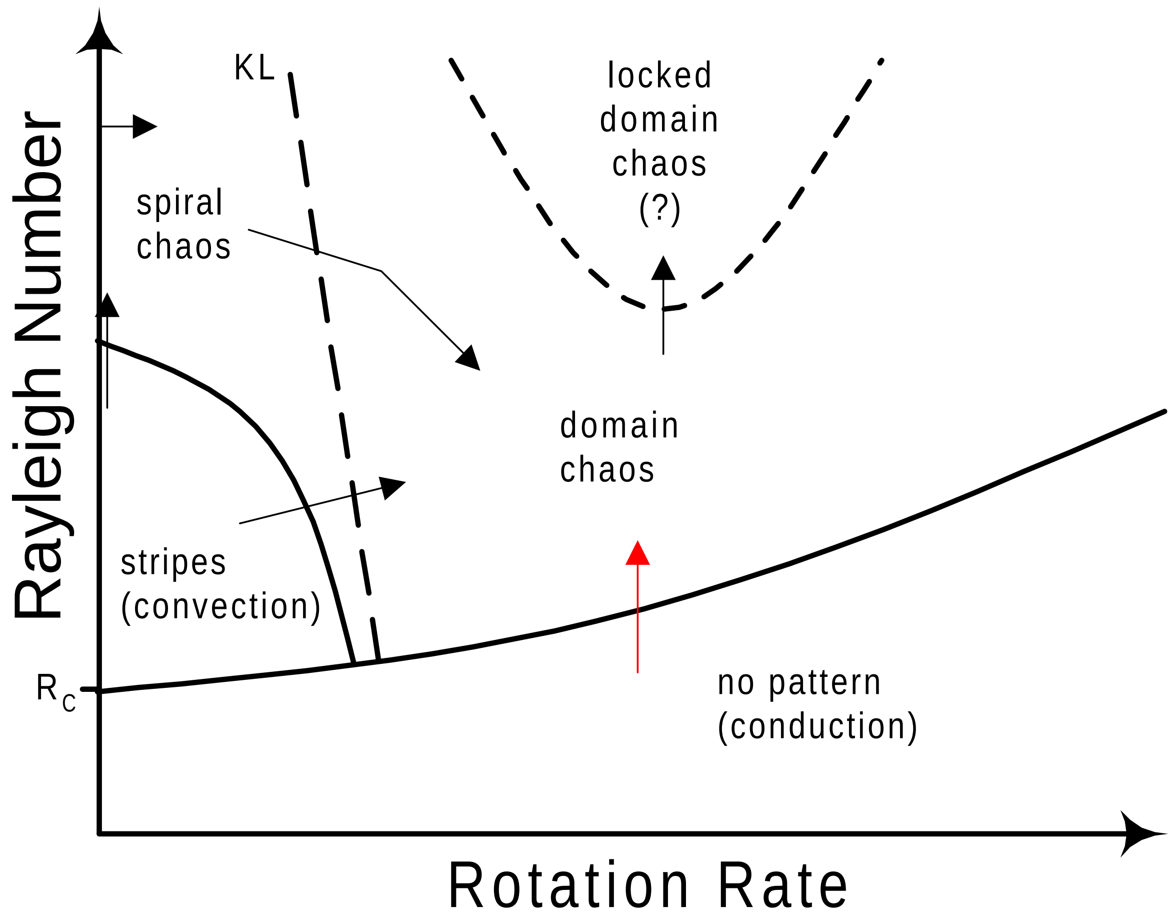

Amplitude equation description (Tu and MCC, 1992)

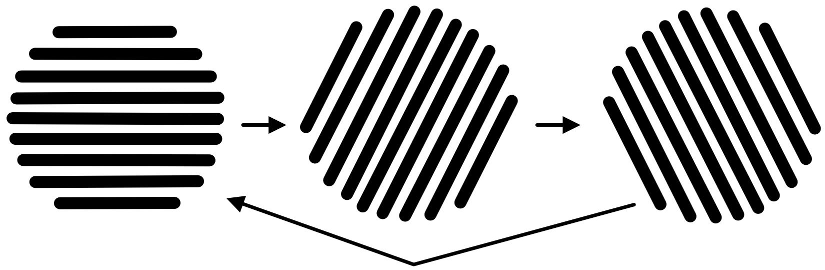

Amplitudes of rolls at 3 orientations $A_i(\mathbf{r}, t),\ i = 1 \ldots 3$

$$\partial_t A_1 = \varepsilon A_1 + \partial^2_{x_1} A_1 - A_1(A_1^2 + g_+ A_2^2 + g_- A_3^2)$$
$$\partial_t A_2 = \varepsilon A_2 + \partial^2_{x_2} A_2 - A_2(A_2^2 + g_+ A_3^2 + g_- A_1^2)$$
$$\partial_t A_3 = \varepsilon A_3 + \partial^2_{x_3} A_3 - A_3(A_3^2 + g_+ A_1^2 + g_- A_2^2)$$

where $\varepsilon = (R - R_c(\Omega)/R_c(\Omega)$

Rescale space, time, and amplitudes:

Rescale $X = \varepsilon^{1/2}x$, $T = \varepsilon t$, $\bar{A} = \varepsilon^{-1/2}A$

$$\partial_T \bar{A}_1 = \bar{A}_1 + \partial_{X_1}^2 \bar{A}_1 - \bar{A}_1(\bar{A}_1^2 + g_+\bar{A}_2^2 + g_-\bar{A}_3^2)$$
$$\partial_T \bar{A}_2 = \bar{A}_2 + \partial_{X_2}^2 \bar{A}_2 - \bar{A}_2(\bar{A}_2^2 + g_+\bar{A}_3^2 + g_-\bar{A}_1^2)$$
$$\partial_T \bar{A}_3 = \bar{A}_3 + \partial_{X_3}^2 \bar{A}_3 - \bar{A}_3(\bar{A}_3^2 + g_+\bar{A}_1^2 + g_-\bar{A}_2^2)$$

Numerical simulations show chaotic dynamics

Therefore in unscaled (physical) units

Length scale $\xi \sim \varepsilon^{-1/2}$

Time scale $\tau \sim \varepsilon^{-1}$

Summary of Tests

Summary of Tests

- Simulations [MCC and Meiron (1994)] of generalized Swift-Hohenberg equations in periodic geometries show results consistent with predictions

Summary of Tests

- Simulations [MCC and Meiron (1994)] of generalized Swift-Hohenberg equations in periodic geometries show results consistent with predictions
- [Hu et al. (1995) + others] Experiments give results that are consistent either with finite values of ξ, τ at onset, or much smaller power laws $\xi \sim \varepsilon^{-0.2}$, $\tau \sim \varepsilon^{-0.6}$

Summary of Tests

- Simulations [MCC and Meiron (1994)] of generalized Swift-Hohenberg equations in periodic geometries show results consistent with predictions
- [Hu et al. (1995) + others] Experiments give results that are consistent either with finite values of ξ, τ at onset, or much smaller power laws $\xi \sim \varepsilon^{-0.2}$, $\tau \sim \varepsilon^{-0.6}$
- [MCC, Louie, and Meiron (2001)] Simulations of generalized Swift-Hohenberg equations in circular geometries of radius Γ gave results consistent with finite size scaling

$$\xi_M = \xi f(\Gamma/\xi) \qquad \text{with} \qquad \xi \sim \varepsilon^{-1/2}$$

Summary of Tests

- Simulations [MCC and Meiron (1994)] of generalized Swift-Hohenberg equations in periodic geometries show results consistent with predictions
- [Hu et al. (1995) + others] Experiments give results that are consistent either with finite values of ξ, τ at onset, or much smaller power laws $\xi \sim \varepsilon^{-0.2}$, $\tau \sim \varepsilon^{-0.6}$
- [MCC, Louie, and Meiron (2001)] Simulations of generalized Swift-Hohenberg equations in circular geometries of radius Γ gave results consistent with finite size scaling

$$\xi_M = \xi f(\Gamma/\xi) \qquad \text{with} \qquad \xi \sim \varepsilon^{-1/2}$$

- [Scheel and MCC, preprint (2005)] Simulations of Rayleigh-Bénard convection with Coriolis forces give $\tau \sim \varepsilon^{-1}$ for small enough ε. For larger ε a slower growth is seen perhaps consistent with $\tau \sim \varepsilon^{-0.7}$.

Summary of Tests

- Simulations [MCC and Meiron (1994)] of generalized Swift-Hohenberg equations in periodic geometries show results consistent with predictions
- [Hu et al. (1995) + others] Experiments give results that are consistent either with finite values of ξ, τ at onset, or much smaller power laws $\xi \sim \varepsilon^{-0.2}$, $\tau \sim \varepsilon^{-0.6}$
- [MCC, Louie, and Meiron (2001)] Simulations of generalized Swift-Hohenberg equations in circular geometries of radius Γ gave results consistent with finite size scaling

$$\xi_M = \xi f(\Gamma/\xi) \qquad \text{with} \qquad \xi \sim \varepsilon^{-1/2}$$

- [Scheel and MCC, preprint (2005)] Simulations of Rayleigh-Bénard convection with Coriolis forces give $\tau \sim \varepsilon^{-1}$ for small enough ε. For larger ε a slower growth is seen perhaps consistent with $\tau \sim \varepsilon^{-0.7}$.
- Scaling of largest Lyapunov exponent consistent with $\lambda \sim c + \varepsilon^{1}$ with c comparable with the finite size shift in onset.

Summary of Tests

- Simulations [MCC and Meiron (1994)] of generalized Swift-Hohenberg equations in periodic geometries show results consistent with predictions
- [Hu et al. (1995) + others] Experiments give results that are consistent either with finite values of ξ, τ at onset, or much smaller power laws $\xi \sim \varepsilon^{-0.2}$, $\tau \sim \varepsilon^{-0.6}$
- [MCC, Louie, and Meiron (2001)] Simulations of generalized Swift-Hohenberg equations in circular geometries of radius Γ gave results consistent with finite size scaling

$$\xi_M = \xi f(\Gamma/\xi) \qquad \text{with} \qquad \xi \sim \varepsilon^{-1/2}$$

- [Scheel and MCC, preprint (2005)] Simulations of Rayleigh-Bénard convection with Coriolis forces give $\tau \sim \varepsilon^{-1}$ for small enough ε. For larger ε a slower growth is seen perhaps consistent with $\tau \sim \varepsilon^{-0.7}$.
- Scaling of largest Lyapunov exponent consistent with $\lambda \sim c + \varepsilon^1$ with c comparable with the finite size shift in onset.
- …

Possible explanations for discrepancies?

- Finite size effects?
- Dislocation glide important (not in Tu-Cross model)?
- Other features of physics important (e.g. continuum of orientations)?
- Centrifugal force important in experimental geometry?
- … or critical-like fluctuation effects important?

Conclusions

Numerical simulations on realistic experimental geometries complement experimental work and yield new insights

- Pattern chaos
  - ◇ Lower noise flows gives consistency of power spectrum with expectation based on deterministic chaos
  - ◇ Visualization of dynamics explains observed power law observed in spectrum
- Mean flow
  - ◇ Confirmed role in $\Gamma \sim 5$ chaos
  - ◇ Importance in spiral defect chaos and shape of stationary patterns
  - ◇ Tends to align rolls normal to boundary (other effects also important)
- Lyapunov exponents and vectors
  - ◇ Positive exponent confirms early experiments were indeed chaotic
  - ◇ Vector may give insight into “mechanism”, e.g. role of defects
  - ◇ Largest exponent scales roughly $\propto \varepsilon$ for domain chaos
- Domain chaos

THE END